

# Transport of Strongly Correlated Electrons

P. Prelovšek\* and X. Zotos†

\**Faculty of Mathematics and Physics, University of Ljubljana, and J. Stefan Institute, 100 Ljubljana, Slovenia*

†*Institut Romand de Recherche Numérique en Physique des Matériaux (EPFL-PPH), CH-1015 Lausanne, Switzerland*

**Abstract.** Lectures deal with the theory of electronic transport, in particular with the electrical conductivity, in systems dominated by strong electron-electron repulsion. The concept of charge stiffness is introduced to distinguish conductors and insulators at  $T = 0$ , but as well usual resistors, possible ideal conductors and ideal insulators at finite temperature. It is shown that the latter singular transport appears in many integrable systems of interacting fermions, the evidence coming from the relation with level dynamics, from the existence of conserved quantities as well as from numerical studies and exact results. Then, exact diagonalization approaches for the calculation of static and dynamical quantities in small correlated systems are described, with the emphasis on the finite-temperature Lanczos method applicable to transport quantities. Finally, anomalous dynamical conductivity within the planar single-band model is discussed in relation with experiments on cuprates.

## INTRODUCTION

In the theory of strongly correlated electrons there are at present still numerous open problems, both regarding the basic understanding of phenomena and even more of the methods of calculation and sensible approximations. Among such theoretical challenges are also electronic transport quantities, such as electrical conductivity, the electronic heat conductivity, the thermopower and the Hall constant. In usual metals and semiconductors the transport theory, based on the Boltzmann semiclassical approach as well as the quantum calculation of relevant scattering mechanisms, involving impurities and electron-phonon coupling, date back to the beginning of then solid state theory. The extension of these methods to strong disorder and strong electron-phonon coupling, introducing the phenomena of localization, polaronic transport etc., using the framework of general linear response theory have been in the focus of theoreticians for several decades. Within the same treatment also the effects of the weak electron-electron coupling has been understood, as summarized within the Landau Fermi liquid concept for electron transport. On the other hand, the strong electron-electron Coulomb repulsion, being the signature of strongly correlated systems, raises new questions of appropriate theoretical techniques and moreover of the basic understanding of the scattering mechanism and its effects.

As a prominent example of the transport quantity we will mainly focus on *the dynamical (optical) electrical conductivity*  $\sigma(\omega)$ , whereby the easiest accessible experimental quantity is the d.c. resistivity  $\rho = 1/\sigma(0)$ . Within the usual Boltzmann theory for a weak electron scattering the relaxation-time approximation represents well the low-frequency

behaviour,

$$\sigma(\omega) = \sigma_0 / (1 + i\omega\tau), \quad (1)$$

where the relaxation time  $\tau$  depends on the particular scattering mechanism and is in general temperature dependent. In the following we will consider only homogeneous systems without any disorder, so the relevant processes in the solid state are electron-phonon scattering and the electron-electron (Coulomb) repulsion. When the latter becomes strong it is expected to dominate also the transport quantities. In this case there appear evidently fundamentally new questions:

a) The repulsion can transform a metal (conductor) into an (Mott-Hubbard) insulator at  $T = 0$  which radically changes transport quantities, both in the ground state as well as at finite temperatures  $T > 0$ .

b) Even in the metallic phase it is not evident which is the relevant scattering process determining  $\tau(T)$  and  $\rho(T)$ . In the absence of disorder and neglecting the electron-phonon coupling the standard theory of purely electron-electron scattering would state that one needs Umklapp scattering processes to yield finite  $\tau$ . That is, the relevant electron Hamiltonian includes the kinetic energy, the lattice periodic potential  $V$  and the electron-electron interaction  $H_{int}$ ,

$$H = H_{kin} + V + H_{int}. \quad (2)$$

Then, in general the electronic current density  $j$  is not conserved due to Umklapp processes in the electron-electron scattering (where the sum of electron momenta is nonzero, equal to nonzero reciprocal wavevector), i.e.  $[H, j] \neq 0$ , leading to the current relaxation and dissipation. The interplay of  $V$  and  $H_{int}$  becomes however quite involved in the case of a strong electron repulsion. This becomes quite clear in examples of integrable tight binding models of interacting fermions, which have anomalous (diverging) transport quantities.

c) Experiments on cuprates, manganites and other novel materials - strange metals - with correlated electrons question the validity of the concept of the current relaxation rate  $1/\tau$ . For example, in cuprates only strongly frequency (and  $T$ ) dependent  $\tau(\omega, T)$  can account for experiments in the normal state, leading to the concept of the marginal Fermi liquid.

In these lectures we will consider only the physics of strongly correlated electrons. The standard framework for theoretical investigations in this case are microscopic tight-binding models for electrons (in general with spin), including the hopping term  $T$  (representing the effect of  $V$  and  $H_{kin}$  and the electron-electron interaction  $H_{int}$

$$\hat{H} = - \sum_{i,j,s} t_{ij} (c_{js}^\dagger c_{is} + H.c.) + H_{int} = T + H_{int}, \quad (3)$$

where  $c_{is} (c_{is}^\dagger)$  are annihilation (creation) operators for fermions on sites  $i$  on a D-dimensional lattice and in most cases  $t_{ij} = t$  is the hopping matrix element between nearest neighbor (n.n.) sites only.  $H_{int}$  is a local (onsite or including only few neighboring sites) interaction defined for specific cases later on.

## LINEAR RESPONSE THEORY

The linear response theory for the electrical a.c. conductivity  $\sigma(\omega)$  has been formulated by Kubo and is standard for dissipative systems [1]. Nevertheless, in correlated systems at  $T = 0$  as well as at  $T > 0$  in particular cases (of integrable models) one has to take in general into account besides the regular part  $\sigma_{reg}(\omega)$  also the singular contribution to the charge dynamical response, i.e.

$$\sigma(\omega) = 2\pi e_0^2 D \delta(\omega) + \sigma_{reg}(\omega), \quad (4)$$

where  $D$  represents the charge stiffness. The analysis in the presence of finite  $D > 0$  as well as the derivation of the proper optical sum rule within the models of correlated electrons (3) requires more care and goes beyond the standard linear response formulations, hence we present it shortly below.

We follow the approach by Kohn [2] introducing a (fictitious) flux  $\phi$  through a torus representing the lattice with periodic boundary conditions (p.b.c.). Such a flux induces a vector potential  $\mathbf{A}$ , being equal on all lattice sites. In lattice (tight-binding) models with a discrete basis for electron wavefunctions the vector potential  $\mathbf{A}$  can be introduced via a gauge transformation (Peierls construction)

$$c_{js}^\dagger \rightarrow c_{js}^\dagger \exp(-ie_0 \mathbf{A} \cdot \mathbf{R}_j), \quad (5)$$

which effectively modifies hopping matrix elements  $t_{ij}$ . Taking  $\mathbf{A}$  as small and assuming that magnetic field does not modify within the lowest order the (local) interaction term  $H_{int}$  one can express the modified tight-binding Hamiltonian (3)

$$\begin{aligned} H(\mathbf{A}) &= - \sum_{i,j,s} t_{ij} e^{-ie_0 \mathbf{A} \cdot \mathbf{R}_{ij}} c_{js}^\dagger c_{is} + H_{int} \approx \\ &\approx H(0) + e_0 \mathbf{A} \cdot \mathbf{j} + \frac{e_0^2}{2} \mathbf{A} \cdot \boldsymbol{\tau} \mathbf{A} = H(0) + H', \end{aligned} \quad (6)$$

where  $\mathbf{R}_{ij} = \mathbf{R}_j - \mathbf{R}_i$  and  $\mathbf{j}$  and  $\boldsymbol{\tau}$  are the current and the stress tensor operators, respectively, given by

$$\begin{aligned} \mathbf{j} &= i \sum_{i,j,s} t_{ij} \mathbf{R}_{ij} c_{js}^\dagger c_{is}, \\ \boldsymbol{\tau} &= \sum_{i,j,s} t_{ij} \mathbf{R}_{ij} \otimes \mathbf{R}_{ij} c_{js}^\dagger c_{is}. \end{aligned} \quad (7)$$

Note that in usual n.n. tight-binding models  $\boldsymbol{\tau}$  is directly related to the kinetic energy operator,  $\tau_{\alpha\alpha} = (H_{kin})_{\alpha\alpha}$ .

The electrical current  $\mathbf{j}_e$  is from the equation (6) expressed as a sum of the particle-current and the diamagnetic contribution,

$$\mathbf{j}_e = -\partial H / \partial \mathbf{A} = -e_0 \mathbf{j} - e_0^2 \boldsymbol{\tau} \mathbf{A}. \quad (8)$$

The above analysis applies also to an oscillating  $\mathbf{A}(t) = \mathbf{A}(\omega) \exp(-i\omega^+ t)$  with  $\omega^+ = \omega + i\delta$  with  $\delta \rightarrow 0$ . This induces an electric field in the system  $\mathbf{E}(t) = -\partial \mathbf{A}(t) / \partial t$ .

We are interested in the response of  $\langle \mathbf{j}_e \rangle(\omega)$ . Evaluating  $\langle \mathbf{j} \rangle$  as a linear response [1] to the perturbation  $H'$  in Eq.(6), and with  $\mathbf{A}(\omega) = \mathbf{E}(\omega)/i\omega^+$ , we arrive at the optical conductivity,

$$\begin{aligned}\tilde{\sigma}(\omega) &= \frac{ie_0^2}{\omega^+N}(\langle \tau \rangle - \chi(\omega)), \\ \chi(\omega) &= i \int_0^\infty dt e^{i\omega^+t} \langle [\mathbf{j}(t), \mathbf{j}(0)] \rangle.\end{aligned}\quad (9)$$

Complex  $\tilde{\sigma}(\omega) = \sigma(\omega) + i\tilde{\sigma}''(\omega)$  satisfies the Kramers-Kronig relation. Since  $\chi(\omega \rightarrow \infty) \rightarrow 0$ , we get from the equation (9) a condition for  $\tilde{\sigma}''(\omega \rightarrow \infty)$ ,

$$\int_{-\infty}^\infty \sigma(\omega) d\omega = \frac{\pi e_0^2}{N} \langle \tau \rangle, \quad (10)$$

which corresponds to the optical sum rule. It reduces to the well known sum rule for continuum electronic systems, as well as for n.n. hopping models where  $\langle \tau_{\alpha\alpha} \rangle = -\langle H_{kin} \rangle / d$  [3]. We can now make contact with the definition (4). From the expression (9) it follows

$$D_{\alpha\alpha} = \frac{1}{2e_0^2} \lim_{\omega \rightarrow 0} \omega \tilde{\sigma}''_{\alpha\alpha}(\omega) = \frac{1}{2N} [\langle \tau_{\alpha\alpha} \rangle - \chi'_{\alpha\alpha}(0)], \quad (11)$$

and

$$\begin{aligned}\sigma_{reg}(\omega) &= \frac{e_0^2}{N\omega} \chi''_{\alpha\alpha}(\omega) = e_0^2 \frac{1 - e^{-\beta\omega}}{\omega} C_{\alpha\alpha}(\omega), \\ C_{\alpha\alpha}(\omega) &= \frac{1}{N} \text{Re} \int_0^\infty dt e^{i\omega t} \langle j_\alpha(t) j_\alpha(0) \rangle.\end{aligned}\quad (12)$$

In any finite system one can write  $C_{\alpha\alpha}(\omega)$  and  $D_{\alpha\alpha}$  in terms of exact eigenstates  $|n\rangle$  with corresponding energies  $\epsilon_n$ ,

$$\begin{aligned}C_{\alpha\alpha}(\omega) &= \frac{1}{N} \sum_{n \neq m} p_n |\langle m | j_\alpha | n \rangle|^2 \delta(\omega - \epsilon_m + \epsilon_n), \\ D_{\alpha\alpha}(\omega) &= \frac{1}{N} [\langle \tau_{\alpha\alpha} \rangle - \sum_{n \neq m} p_n \frac{|\langle m | j_\alpha | n \rangle|^2}{\epsilon_m - \epsilon_n}],\end{aligned}\quad (13)$$

where  $p_n = e^{-\beta\epsilon_n}/Z$  is the Boltzmann weight of each level and  $Z = \sum_n e^{-\beta\epsilon_n}$  is the thermodynamic sum.

## Conductors and insulators

### *Ground state*

At  $T = 0$  the charge stiffness  $D_{\alpha\alpha}^0 = D_{\alpha\alpha}(T = 0)$  is the central quantity determining the charge transport. As already formulated by Kohn [2]  $D^0$  can be expressed directly as

a sensitivity of the ground state to the applied flux  $\phi_\alpha = eA_\alpha$ ,

$$D_{\alpha\alpha}^0 = \frac{1}{2N} \frac{\partial^2 E_0}{\partial \phi_\alpha^2} \Big|_{\phi_\alpha=0}. \quad (14)$$

Since at  $T = 0$  there cannot be any dissipation and one expects  $\sigma_{reg}(\omega \rightarrow 0) = 0$ , we have to deal with two fundamentally different possibilities with respect to  $D^0$  (for simplicity we consider an isotropic tensor  $\mathbf{D}^0$ ):

a)  $D^0 > 0$  is characteristic for a *conductor* or *metal*,

b)  $D^0 = 0$  applies to an *insulator*, which can have the origin in the filled band of electrons (usual band insulator) or for non-filled band in the Mott-Hubbard mechanism due to strong electron repulsion, i.e. electron correlations. The latter situation is clearly of interest here. Note that the same criterion of the sensitivity to flux has been applied to disordered systems, relevant to the theory of the electron localization.

The theory of the metal-insulator transition solely due to the Coulomb repulsion (Mott transition) has been intensively investigated in last decades and is one of better understood parts of the physics of strongly correlated electrons. The emphasis has been on analytical and numerical studies of particular models of correlated electrons. The prototype and the most investigated model in this context is the Hubbard model with the onsite repulsion,

$$H_{int} = U \sum_i n_{i\uparrow} n_{i\downarrow}. \quad (15)$$

Let us consider as an example the Hubbard model on a one dimensional (1D) chain with  $L$  sites. We first derive the result for free fermions at  $U = 0$ . The eigenvalues in the presence of a flux  $\phi$  become  $\epsilon_k = -2t \cos(k + \phi)$  giving:

$$E_0 = -4t \sum_{|k| < k_F} \cos(k + \phi), \quad k = 2\pi \text{ integer}/L. \quad (16)$$

Following Eq.(14) we get

$$D^0 = -\frac{1}{L} \langle 0 | T | 0 \rangle = \frac{2t}{\pi} \sin k_F = \frac{2t}{\pi} \sin \frac{\pi n}{2}, \quad (17)$$

where  $n$  is the density of fermions ( $n = 2k_F/\pi$ ). We notice that  $D$  vanishes for an empty band  $n = 0$ , i.e.  $D^0 \simeq tn$  for  $n \rightarrow 0$ , and for a filled band  $n = 2$  where  $D^0 \simeq t(2 - n)$  for  $n \rightarrow 2$ .  $D^0$  is maximum at half filling where  $D^0(n = 1) = 2t/\pi$ .

Another simple limit is  $U = \infty$ . Since in this case the double occupation of sites is forbidden due to Eq.(15), i.e.  $n_{i\uparrow} n_{i\downarrow} = 0$ , fermions behave effectively as spinless and the result is

$$D^0 = \frac{t}{\pi} |\sin(\pi n)|, \quad (18)$$

and in contrast to noninteracting case  $D^0$  vanishes at half filling, i.e.  $D^0 \simeq t|1 - n|$  for  $n \rightarrow 1$ .

Analytical results in 1D indicate that  $D^0 = 0$  at half filling persists in the Hubbard model at all  $U > 0$ , whereby the dependence  $D(n)$  is between both limits  $U = 0$  and  $U = \infty$ . The insulating state at half filling is a generic feature also for a wider class of other 1D models, as the  $t$ - $V$  model (equivalent to the anisotropic Heisenberg model), the  $t$ - $J$  model etc.

The metal - insulator transition in higher dimensions is more difficult and open subject and there are no exact analytical results [4]. Still it is established that in the 2D Hubbard model there is an insulator at half filling for arbitrary  $U$  due to the nesting of the Fermi surface. The insulating character is explicitly evident also within the 2D  $t$ - $J$  model, which represents the large  $U$  limit of the Hubbard model. The metal - insulator transition has been also extensively studied in the limit of infinite dimensions [5]. One would like to know the behavior of weakly doped Mott-Hubbard insulator at  $n < 1$ . Numerical results for  $D$  on Hubbard model as well as the  $t$ - $J$  model in 2D seem to indicate linear variation  $D \propto (1 - n)^\alpha$  with  $\alpha = 1$  [6], but there are also arguments for  $\alpha > 1$  [4].

### *Finite Temperature*

At  $T > 0$  there are in principle more possibilities, since we have to deal with  $\tilde{\sigma}_0 = \sigma_{reg}(\omega \rightarrow 0) \geq 0$  as well as with  $D(T) \geq 0$  [7]:

a) *Normal conductor* or *resistor* has a nonsingular response, i.e.  $D = 0$ , and a finite conductivity (resistivity)  $\tilde{\sigma}_0 > 0$ .

b)  $D(T) > 0$  would be a signature of an *ideal conductor*, which in analogy to  $T = 0$  does not show any Ohm's energy dissipation, but rather a reactive response (acceleration) of the charge in an applied external electric field. In this case  $\tilde{\sigma}_0$  is irrelevant since a singular  $D > 0$  term dominates at low  $\omega$ . We will see that such a case is realized in a number of nontrivial integrable many-fermion models.

c) The situation with  $D(T) = 0$  and  $\tilde{\sigma}_0 = 0$  would correspond to an *ideal insulator*, since there will not be no conduction in spite of  $T > 0$ . This is clearly a very unusual possibility, for which so far at least indications exist in integrable systems [7].

## **TRANSPORT AND INTEGRABILITY**

It is plausible that integrable systems can have anomalous transport properties. In classical systems this observation is well established. On the other hand, the proposition that integrable quantum many-body systems show dissipationless transport at finite temperatures is rather recent [8]. The key to this idea comes from a study of the Drude weight at finite temperatures  $D(T > 0)$ . Since all integrable many-body fermionic models are in 1D, we will further restrict ourselves to 1D, although some statements are more general.

## Transport and level dynamics

It is convenient to discuss  $D(T)$  with a generalization of the original Kohn's approach [2] for zero temperature, by relating  $D(T)$  to the thermal average of curvatures  $D_n$  of energy levels  $\epsilon_n$  subject to the fictitious flux  $\phi = eA$ . Since the flux induces the perturbation  $H' = -\phi j$ , we can expand the eigenenergies  $\epsilon_n(\phi)$  up to the second order in  $\phi$ ,

$$\epsilon_n(\phi) = \epsilon_n(0) - \phi \langle n | j | n \rangle + \frac{1}{2} \langle n | j | n \rangle + \phi^2 \sum_{m \neq n} \frac{|\langle m | j | n \rangle|^2}{\epsilon_m - \epsilon_n}. \quad (19)$$

Following Eq.(13)) we can then write  $D(T)$  as

$$D = \frac{1}{L} \sum_n p_n D_n = \frac{1}{2L} \sum_n p_n \frac{\partial^2 \epsilon_n(\phi)}{\partial \phi^2} \Big|_{\phi \rightarrow 0}, \quad (20)$$

i.e. in analogy to  $T = 0$  case  $D$  can be expressed in terms of curvatures of levels, at  $T > 0$  weighted with their Boltzmann factors.

Evaluating the second derivative of the free energy  $F$  as a function of flux  $\phi$ , we also find

$$\frac{\partial^2 F}{\partial \phi^2} = 2D - \beta \sum_n p_n \left( \frac{\partial \epsilon_n}{\partial \phi} \right)^2 + \left( \sum_n p_n \frac{\partial \epsilon_n}{\partial \phi} \right)^2. \quad (21)$$

In this expression the third term vanishes by symmetry and in a system as ours without persistent currents,  $\partial^2 F / \partial \phi^2$  has to vanish in the thermodynamic limit. Therefore in the  $L \rightarrow \infty$  limit the charge stiffness can be alternatively represented as

$$D = \frac{\beta}{2L} \sum_n p_n \left( \frac{\partial \epsilon_n}{\partial \phi} \right)^2. \quad (22)$$

On the other hand, we know from rather recent studies that the integrability of a system is reflected in the distribution of level spacings  $P(s)$  [9]. For *integrable systems*  $P(s)$  follows the *Poisson distribution*  $P(s) \propto \exp(-s)$ , while in *non-integrable systems* the *Gaussian orthogonal ensemble* (GOE) one given by the Wigner surmise,  $P(s) \propto s \exp(-s^2)$ . The difference is due to the existence of a macroscopic number of conservation laws in integrable systems that, allowing level crossing, suppresses level repulsion. As for the behavior of  $D$ , we can now argue that in non-integrable systems, due to the level repulsion, the levels move as a function of  $\phi$  in an energy spacing of the order of the inverse of the many-body density of states. The latter becomes exponentially small with increasing  $L$ , leading to an exponential suppression of slopes  $\partial \epsilon_n / \partial \phi$  as well as  $D(T)$ . On the other hand, in the integrable system, the slopes due to the absence of level repulsion can take values of the order of one and  $D(T)$  can remain finite even in the thermodynamic limit.

In non-integrable systems the assumption of the random matrix theory has also other consequences. In particular, there exists a relation between off-diagonal and diagonal

elements [10]

$$\langle |j_{nm}|^2 \rangle_{\varepsilon_n \neq \varepsilon_m} = \langle (j_{nm} - \bar{v}(E))^2 \rangle = \sigma^2(E). \quad (23)$$

Here  $j_{nm} = \langle n | j | m \rangle$ ,  $\bar{v} = \langle j_{nn} \rangle$  and the outer brackets denote an average of matrix elements locally in the spectrum. This leads for a normal resistor with  $D(T > 0) = 0$  to the relation for the d.c. conductivity,

$$\sigma_0 = \beta \pi e^2 \sum_{n \neq m} p_n |j_{nm}|^2 \delta(\varepsilon_n - \varepsilon_m) = \frac{\beta \pi e^2}{2} \int_{-\infty}^{\infty} \frac{\exp(-\beta E)}{Z} \rho^2(E) \sigma^2(E) dE. \quad (24)$$

$\sigma_0$  can be thus expressed in terms of  $\sigma(\varepsilon)$ , which measures the sensitivity to flux (velocity of level dynamics). Such an approach has been used already in the theory of conduction in disordered systems.

## Models

### *Particle in a fermionic bath*

The first model we study is a toy model of dissipation. The Hamiltonian describing a single (tagged) particle interacting with a bath of spinless fermions is

$$H = -t_h \sum_i (e^{i\phi} d_{i+1}^\dagger d_i + H.c.) - t \sum_i (c_{i+1}^\dagger c_i + H.c.) + U \sum_i d_i^\dagger d_i c_i^\dagger c_i, \quad (25)$$

where  $c_i (c_i^\dagger)$  are operators for spinless fermions (without charge, i.e. not sensitive to the flux) and  $d_i (d_i^\dagger)$  for the tagged particle on a chain with p.b.c. The interaction comes only through the on-site repulsion  $U > 0$ . The current  $j$  refers to the tagged particle only,

$$j = -it_h \sum_i d_{i+1}^\dagger d_i + H.c. \quad (26)$$

and is not conserved for  $U > 0$ , i.e.  $[j, H] \neq 0$ . In this model the conductivity  $\sigma(\omega)$  corresponds to the mobility  $\mu(\omega)$  of the tagged particle. The model (25) is integrable by the Bethe ansatz method in the case of equal masses, i.e.  $t_h = t$  (where it is equivalent to the problem of a Hubbard chain in a nearly polarized state  $S^z = S_{max}^z - 1$ ) and non-integrable for unequal masses  $t_h \neq t$ .

In Fig. 1 we present  $D(T)$  as a function of  $t_h/t$  [8], for different  $T$  and  $L$  but for fixed  $U/t = 2$  at half-filled band of spinless electrons  $N_e = L/2$ . Results clearly reveal:

a) a nonmonotonic behavior of  $D(T)$  as we sweep through the integrable  $t_h = t$  point for  $T > 0$ ,

b) a very weak dependence of  $D(T)$  on the system size  $L$  for the integrable case  $t_h = t$ , and on contrary a rather strong one for the non-integrable ones.

To obtain an impression of the overall behavior of  $D(T)$  as a function of  $T$ , we present in Fig. 2  $D(T)/D_0$  for  $t_h/t = 1.0, 0.5$  and different size systems.



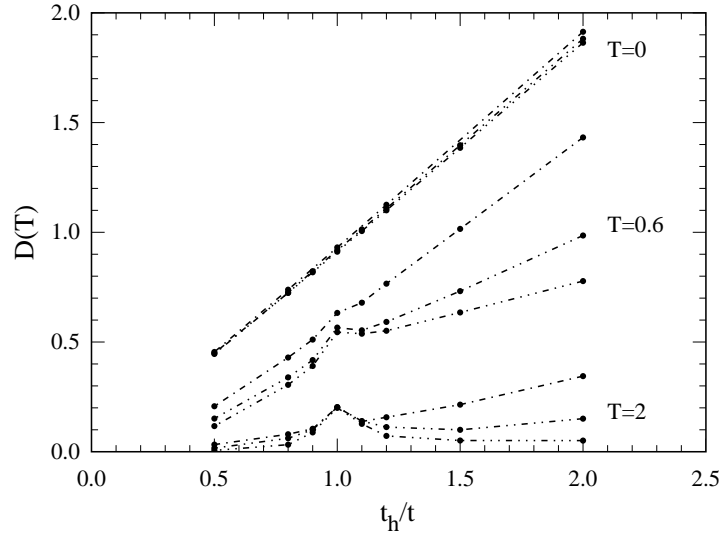


**FIGURE 1.**  $D(T)/D_0$  as a function of  $t_h/t$  for  $U/t = 2$ , different temperatures  $T$  and system sizes  $L$ :  $(-\cdot-)$   $L = 6$ ,  $(-\cdot\cdot-)$   $L = 10$ ,  $(-\cdot\cdot\cdot-)$   $L = 14$ .

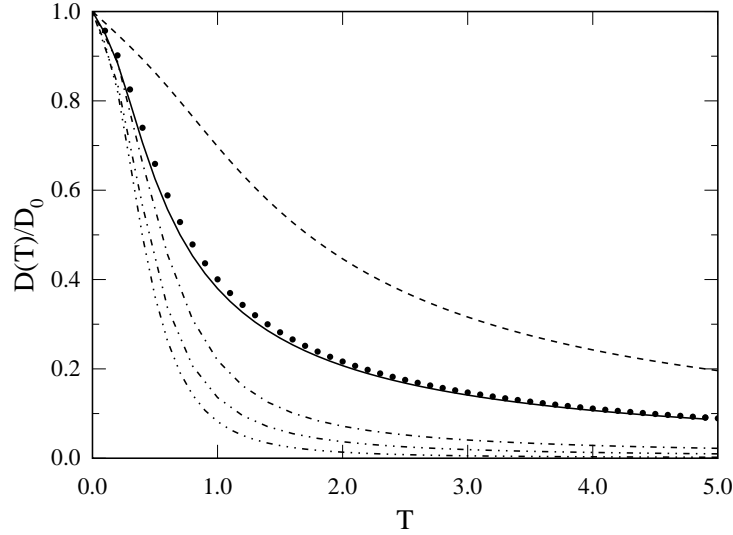


**FIGURE 2.**  $D(T)/D_0$  as a function of  $T$  for  $U/t = 2$ . Numerical results are indicated by  $(-\cdot-)$   $L = 6$ ,  $(-\cdot\cdot-)$   $L = 10$ ,  $(-\cdot\cdot\cdot-)$   $L = 14$  and  $t_h = 0.5t$ ; by points for  $t_h = t$  and  $L = 18$ . The continuous line is the Bethe ansatz result and the dashed line  $D(T)/D_0$  for a free particle.

Above results are clearly consistent with the conjecture [8] that at the integrable point  $t_h = t$  we are dealing with ideal conductance (tagged particle mobility) with  $D(T > 0) > 0$ , while for  $t_h \neq t$  the transport is “normal” with  $D(T > 0) = 0$  and finite d.c. mobility  $\mu_0$ . A very relevant but so far open question is how does  $\mu_0$  behave close to the integrable point, where it diverges. One would speculate on the power law divergence  $\mu_0 \propto |t - t_h|^{-\gamma}$  with  $\gamma > 1$ , which is partly supported by numerical results [11].

### *t-V model*

In contrast to the system of a single particle in a bath the second model, i.e. the generalized *t-V* model, is a simplest model of a homogeneous system of interacting spinless fermions

$$H = -t \sum_{i=1}^L (e^{i\phi} c_{i+1}^\dagger c_i + H.c.) + V \sum_{i=1}^L n_i n_{i+1} + W \sum_{i=1}^L n_i n_{i+2}, \quad (27)$$

where the interaction is between fermions on the n.n. sites (*V* term) as well as next n.n. sites (*W* term). This Hamiltonian is integrable using the Bethe ansatz method for  $W = 0$  and non-integrable for  $W \neq 0$ . For  $W = 0$  and  $V < 2t$  the ground state is metallic, while for  $V > 2t$  a charge gap opens at half filling  $n = 1/2$  and the system is an insulator. For  $W = 0$  the *t-V* model is equivalent to the Heisenberg spin 1/2 chain as it can be shown using a Jordan-Wigner transformation.

We studied numerically [7] various size systems with p.b.c. and  $N_e = L/2$  fermions (half-filled band). In order to avoid an artificial smoothing procedure of the discrete  $\sigma(\omega)$  spectra of our finite size systems, it is convenient to present the integrated and normalized intensity  $I(\omega)$

$$I(\omega) = D^* + \frac{2L}{\langle -T \rangle} \int_{0+}^{\omega} d\omega' \sigma(\omega'), \quad D^* = \frac{2LD}{\langle -T \rangle}. \quad (28)$$

We show in Fig. 3  $I(\omega)$  and  $D^*$  for a non-integrable case with  $W \neq 0$ . Indeed, as expected for a generic metallic conductor (resistor), we find that  $D^*$  scales to zero, probably exponentially with system size  $L$ . At the same time  $\sigma_0 > 0$  as  $I(\omega)$  approaches  $\omega = 0$  with a finite slope. These two results imply that the non-integrable system indeed behaves as a normal conductor at  $T > 0$ .

In contrast to the non-integrable case the behavior of  $I(\omega)$  for an integrable system, as shown in Fig. 4, is totally different. In order to study the finite size dependence of the charge stiffness, we plot in the inset  $D^*$  as a function of  $1/L$ ; the dashed lines indicate a 3<sup>rd</sup> order polynomial extrapolation based on the  $L = 8, 12, 16$  site systems, suggested by the very good agreement obtained with the  $T = 0$  analytical result.

We find that for  $L \rightarrow \infty$  the extrapolated  $D^* \neq 0$ . At the same time  $\sigma_0 = \sigma(\omega \rightarrow 0) \rightarrow 0$  as  $I(\omega)$  seems to approach  $\omega = 0$  with zero slope. This behavior is reminiscent of a pseudogap. These two results indicate that the integrable system behaves as an *ideal conductor* at  $T > 0$ . Moreover we find that the normalized  $D^*$  approaches a nontrivial finite value  $D_\infty^*$  in the limit  $T \rightarrow \infty$ , depending on  $V/t$  and on band filling, as both  $D$  and  $\langle -T \rangle$  are proportional to  $\beta$  in this limit.

Finally, as we mentioned in the introduction, the integrability is expected to have an effect also in a ‘‘Mott-Hubbard’’ insulating state. In the traditional scenario, the insulator at zero temperature is characterized by  $D_0 = 0$  and  $\sigma_0 = 0$ ; at finite temperatures  $T > 0$ ,  $D(T)$  remains zero but due to thermally activated conduction,  $\sigma_0 > 0$ . As we will show below this scenario seems to be verified in the generic non-integrable systems but not in the integrable ones.

The test case is the integrable *t-V* model ( $W = 0$ ) at half-filling  $n = 1/2$ , but in the insulating regime  $V > 2t$ . The ground state here is insulating characterized by  $D_0 = 0$  and

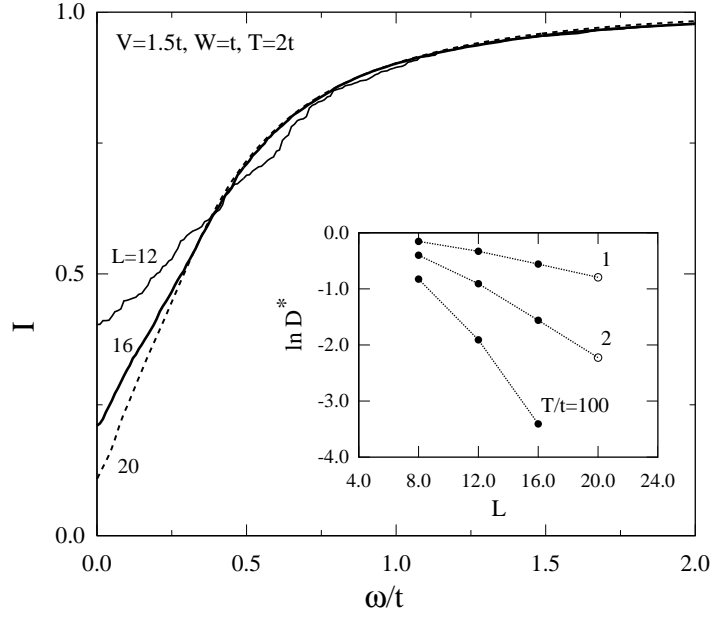


**FIGURE 3.** Integrated conductivity  $I(\omega)$  for  $V = 1.5t, W = t, T = 2t$ , for  $L = 12, 16$  (exact diagonalization - full lines) and  $L = 20$  (Lanczos method - dotted lines). In the inset  $\ln D^*$  vs.  $L$  is plotted: exact diagonalization (disks),  $T > 0$  Lanczos method (circles).

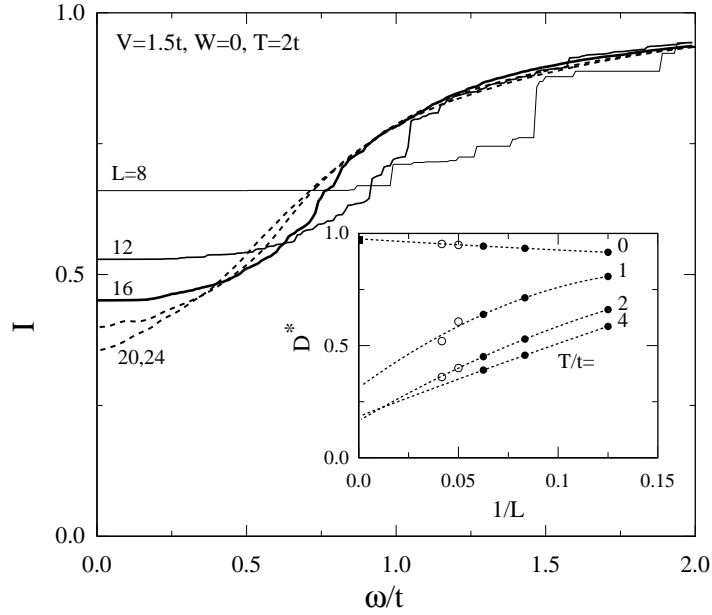


**FIGURE 4.** Integrated conductivity  $I(\omega)$  for  $V = 1.5t, W = 0, T = 2t$ , for  $L = 8 - 16$  (exact diagonalization - full lines) and  $L = 20, 24$  (Lanczos method - dotted lines). Inset shows normalized charge stiffness  $D^*$  vs.  $1/L$ : exact diagonalization (disks),  $T > 0$  Lanczos method (circles), analytical result (square) and 3<sup>rd</sup> order polynomial extrapolation from  $L = 8, 12, 16$  (dotted line).

a finite charge gap. Numerical results at finite temperatures [7]  $D^*(T > 0) = I(\omega = 0)$  seems also to *decrease* exponentially with the system size scaling to zero for  $L \rightarrow \infty$ . This precludes a possibility for ideal conductivity at  $T > 0$ . Furthermore  $I(\omega)$  seems to approach  $\omega = 0$  with a zero slope, showing a depletion of weight within a low frequency region of order  $\omega < t$ . These are characteristics of an *ideal insulator*, not conducting even at high temperatures  $T \gg \Delta_0$ .

In contrast, non-integrable systems of roughly the same charge gap exhibit a qualitatively different behavior.  $I(\omega)$  approaches  $\omega = 0$  with finite (although small) slope, consistent with a small static conductivity  $\sigma_0 > 0$ , consistent with the conduction due to electron - hole pairs, thermally activated over the charge gap.

## Transport and conservation laws

The integrable quantum many-body systems, as the Heisenberg spin 1/2 chain or the one dimensional Hubbard model, are characterized by a macroscopic number of conserved quantities. It is natural to think that the singular transport behavior is related to the existence of such conserved quantities. A set of them is represented by local operators  $Q_n$ , commuting with each other  $[Q_n, Q_m] = 0$  and with the Hamiltonian,  $[Q_n, H] = 0$ . The index  $n$  indicates that the operator  $Q_n$  is of the form  $Q_n = \sum_{l=1}^L q_l^n$ , where  $q_l^n$  are local operators involving  $n$  sites around site  $l$ , on a lattice of  $L$  sites.

The physical content of  $Q_n$  is not clear in general. Nevertheless, for different models discussed below, the first nontrivial quantity  $Q_3$  ( $Q_2$  is the Hamiltonian) has a simple physical significance. It is equal or closely related to the energy current operator  $j^E$ . Through its coupling to the current operator  $j$  it gives an alternative explanation for the singular  $D(T > 0) > 0$ .

The time decay of correlations is related to conserved quantities in a Hamiltonian system by an inequality introduced by Mazur[12, 13]

$$\lim_{T \rightarrow \infty} \frac{1}{T} \int_0^T \langle A(t)A \rangle dt \geq \sum_n \frac{\langle A Q_n \rangle^2}{\langle Q_n^2 \rangle}, \quad (29)$$

which is based on a general positivity of spectra which hold for stationary processes. Here, operators are assumed hermitian,  $A^\dagger = A$ , and  $\langle \rangle$  denotes the thermodynamic average. The left hand side can be written as a sum of a time-independent constant  $\tilde{D}$  and a time-dependent (decaying) function  $C(t)$ , expressed in terms of eigenstates,

$$\begin{aligned} \langle A(t)A \rangle &= \sum_{n,m(\epsilon_m=\epsilon_n)} p_n |\langle n|A|m \rangle|^2 + \sum_{n,m(\epsilon_m \neq \epsilon_n)} p_n |\langle n|A|m \rangle|^2 e^{i(\epsilon_n - \epsilon_m)t} \\ &= \tilde{D} + C(t). \end{aligned} \quad (30)$$

For time correlations  $\langle A(t)A \rangle$  with a non-singular low frequency behavior the second term  $\lim_{T \rightarrow \infty} \frac{1}{T} \int_0^T C(t)dt$  goes to zero and therefore

$$\tilde{D} \geq \sum_n \frac{\langle A Q_n \rangle^2}{\langle Q_n^2 \rangle}. \quad (31)$$

We can use this inequality for the analysis of  $\sigma(\omega)$  related to the current-current correlation  $\langle j(t)j \rangle$ . Charge stiffness  $D$ , Eq.(22), in this case is directly related to  $\tilde{D}$ , and we get

$$D \geq \frac{\beta}{2L} \sum_n \frac{\langle JQ_n \rangle^2}{\langle Q_n^2 \rangle}. \quad (32)$$

In this derivation we assume that the regular part  $\sigma_{reg}(\omega)$  shows a non-singular behavior at low frequencies so that the contribution from  $C(t)$  in (29) vanishes. The latter is consistent with numerical simulations showing for integrable systems a pseudogap at small  $\omega$  and so a vanishing regular part  $\sigma_{reg}(\omega \rightarrow 0)$ .

In general it is difficult to evaluate the right hand side of the inequality (29) involving the “overlap”  $\langle AQ_n \rangle$ . However, in some examples presented below, this correlation can easily be evaluated in the case of a grand canonical trace over states, in the thermodynamic limit and for  $\beta \rightarrow 0$ .

Before studying concrete models we construct the energy current operator  $j^E$  for tight-binding models with n.n. hopping only, where the Hamiltonian can be presented as a sum

$$H = \sum_{i=1}^L h_{i,i+1}. \quad (33)$$

where  $h_{i,i+1}$  are local energy operators acting on a bond.  $H$  is a conserved quantity, hence the time evolution of the local  $h_{i,i+1}$  can be written as the divergence of energy current operator  $j_i^E$ :

$$\frac{\partial h_{i,i+1}}{\partial t} = i[H, h_{i,i+1}] = -(j_{i+1}^E - j_i^E), \quad (34)$$

and we get for the (total) energy current

$$j^E = \sum_{i=1}^L j_i^E = -i \sum_{i=1}^L [h_{i-1,i}, h_{i,i+1}]. \quad (35)$$

### *t-V model: Heisenberg model*

*t-V* model is through the through a Jordan-Wigner transformation equivalent to the anisotropic Heisenberg spin ( $S = 1/2$ ) Hamiltonian, provided that  $J_x = J_y$ ,

$$H = \sum_{i=1}^L [J_x S_i^x S_{i+1}^x + J_y S_i^y S_{i+1}^y + J_z S_i^z S_{i+1}^z]. \quad (36)$$

Here the local energy current operators  $j_i^E$  can be expressed as

$$j_i^E = J_x J_y (xzy - yzx)_{i-1,i+1} + J_y J_z (yxz - zxy)_{i-1,i+1} + J_z J_x (zyx - xyz)_{i-1,i+1}, \quad (37)$$

with  $(\alpha\beta\gamma - \gamma\beta\alpha)_{i-1,i+1} = S_{i-1}^\alpha S_i^\beta S_{i+1}^\gamma - S_{i-1}^\gamma S_i^\beta S_{i+1}^\alpha$ .

It is straightforward to verify that the global energy current operator  $j^E$  commutes with the  $H$  (36) and coincides with  $Q_3$ . Consistent with the notation  $Q_2$  for the Hamiltonian is the sum of local operators involving two sites  $q_2 = h_{i,i+1}$ ,  $q_i^3 = j_i^E$  involves three neighboring sites etc.

The vanishing commutator  $[j^E, H] = 0$  implies also that the energy current time correlations are independent of time. The non-decaying of the energy current then leads evidently to a *singular thermal conductivity*  $\kappa$  related to the  $\langle j^E(t) j^E \rangle$  correlation as well as a *singular thermopower* related to  $\langle j^E(t) j \rangle$ .

In the language of the fermionic  $t$ - $V$  model  $j^E$  is given by

$$j_i^E = t^2(ic_{i+1}^\dagger c_{i-1} + h.c.) + V j_{i,i+1}(n_{i-1} + n_{i+2} - 1), \quad (38)$$

where  $j_{i,i+1} = t(ic_{i+1}^\dagger c_i + h.c.)$  is the local particle current. From (32) one can get an explicit expression for  $\beta \rightarrow 0$ , where the leading order of the high- $T$  expansion of  $\langle j^E j \rangle$  and  $\langle jj \rangle$  yields

$$D \geq \frac{\beta}{2} \frac{2V^2 n(1-n)(2n-1)^2}{1 + V^2(2n^2 - 2n + 1)}. \quad (39)$$

We note that outside the half-filling  $n \neq 1/2$ ,  $D > 0$  implies again an ideal conductivity as shown before using the argument of a relation to the level dynamics. For  $n = 1/2$  the inequality is however insufficient for proving that  $D$  is nonzero. Due to the electron-hole symmetry, this remains true even if we consider all higher order conserved quantities  $Q_n$ . This evidently presents an open problem, since the inequality seems to be exhausted neglecting possible nonlocal conserved quantities.

### Hubbard model

As above one can define a local energy operator for the Hubbard model,

$$h_{i,i+1} = -t \sum_s (c_{is}^\dagger c_{i+1,s} + h.c.) + \frac{U}{2} \left[ (n_{i\uparrow} - \frac{1}{2})(n_{i\downarrow} - \frac{1}{2}) + (n_{i+1\uparrow} - \frac{1}{2})(n_{i+1\downarrow} - \frac{1}{2}) \right], \quad (40)$$

and

$$j_i^E = \sum_s t^2 (ic_{i+1,s}^\dagger c_{i-1,s} + h.c.) - \frac{U}{2} (j_{i-1,i,s} + j_{i,i+1,s})(n_{i,-s} - \frac{1}{2}), \quad (41)$$

where  $j_{i,i+1,s} = (-t)(-ic_{i+1,s}^\dagger c_{is} + h.c.)$  is the particle current. By comparing the expression for  $j^E$  to  $Q_3$ , we find that they coincide when the factor  $U/2$  in (41) is replaced by  $U$ . One can verify that the energy current  $j^E$  has a finite overlap  $\langle j^E Q_3 \rangle$ , with the

conserved quantity  $Q_3$ . We therefore conclude that although the energy current correlations are time dependent still they do not decay to zero so that the thermal transport coefficients are singular.

Using again (32) we find for the charge stiffness  $D$  of the Hubbard model, again at  $\beta \rightarrow 0$ ,

$$D \geq \frac{\beta}{2} U^2 \frac{\sum_s n_s (1 - n_s) (2n_{-s} - 1)}{2 \sum_s n_s (1 - n_s) [1 + (U/2)^2 (2n_{-s}^2 - 2n_{-s} + 1)]}, \quad (42)$$

where  $n_s$  are densities of  $s = \uparrow, \downarrow$  fermions. Again, we get  $D(T) > 0$  outside half filling  $n_s \neq 1/2$ . On the other hand  $D(T) = 0$  for  $n_s = 1/2$ . In the latter case the validity or deficiency of the result is not so clear, since the insulating  $D = 0$  at half filling is not unexpected and there are so far also no reliable analytical or numerical result which could be confronted with the one following from the Mazur inequality.

## NUMERICAL METHODS

Let us turn to the discussion of higher-dimensional (as well as nonintegrable 1D) correlated systems which behave as normal metals with finite d.c. transport quantities, e.g. the resistivity  $\rho(T)$ . It is evident that the evaluation of  $\sigma_0(T)$  via the linear response theory requires the method at  $T > 0$ .

The absence of well-controlled analytical approaches to models of strongly correlated electrons has stimulated the development of computational methods. Conceptually the simplest is the exact diagonalization method of small systems [6]. In models of correlated electrons, however, one is dealing with the number of quantum basis states  $N_{st}$  which grows exponentially with the size of the system. Within the Hubbard model there are 4 basis states for each lattice site, therefore the number of basis states in the  $N$ -site system is  $N_{st} \propto 4^N$ . In the  $t$ - $J$  model  $N_{st}$  still grows as  $\propto 3^N$ , and within the  $t$ - $V$  (or Heisenberg) model as  $\propto 2^N$ . In the exact diagonalization of such systems one is therefore representing operators with matrices  $N_{st} \times N_{st}$ , which become large already for very modest values of  $N$ .

One straightforward approach to dynamics at  $T > 0$  is to perform full diagonalization of small system, calculating all eigenstates and eigenfunctions  $\epsilon_n, |n\rangle$ , required to evaluate matrix elements, e.g.  $\langle n|j|m\rangle$ . At the present status of computers we are restricted to diagonalization of matrices with  $N_{st} < 3000$ , so that reachable systems are  $N \leq 16$ ,  $N \leq 12$ ,  $N \leq 8$  for the  $t$ - $V$  model, the  $t$ - $J$  model and the Hubbard model, respectively.

### Lanczos method

The helpful circumstance is that for most interesting operators and lattice models only a small proportion of matrix elements is nonzero within the local basis. Then, the operators can be represented by sparse matrices with  $N_{st}$  rows and at most  $f(N)$  nonzero elements in each row. In this way memory requirements are relaxed and matrices up to  $N_{st} \sim 10^8$  are considered in recent applications. Finding eigenvalues and eigenvectors

of such large matrices is not possible with standard algorithms performing the full diagonalization. One must instead resort to power algorithms, among which the Lanczos algorithm is one of the most widely known [14]. It is mainly used for the calculation of the ground state of a finite system, i.e. the ground-state energy  $E_0$  and wavefunction  $|\Psi_0\rangle$ .

The Lanczos algorithm [14] starts with a normalized random vector  $|\phi_0\rangle$  in the vector space in which the Hamiltonian operator  $H$  is defined.  $H$  is applied to  $|\phi_0\rangle$  and the resulting vector is split in components parallel to  $|\phi_0\rangle$ , and  $|\phi_1\rangle$  orthogonal to it, respectively,

$$H|\phi_0\rangle = a_0|\phi_0\rangle + b_1|\phi_1\rangle. \quad (43)$$

Since  $H$  is Hermitian,  $a_0 = \langle\phi_0|H|\phi_0\rangle$  is real, while the phase of  $|\phi_1\rangle$  can be chosen so that  $b_1$  is also real. In the next step  $H$  is applied to  $|\phi_1\rangle$ ,

$$H|\phi_1\rangle = b'_1|\phi_0\rangle + a_1|\phi_1\rangle + b_2|\phi_2\rangle, \quad (44)$$

where  $|\phi_2\rangle$  is orthogonal to  $|\phi_0\rangle$  and  $|\phi_1\rangle$ . It follows also  $b'_1 = \langle\phi_0|H|\phi_1\rangle = b_1$ . Proceeding with the iteration one gets in  $i$  steps

$$H|\phi_i\rangle = b_i|\phi_{i-1}\rangle + a_i|\phi_i\rangle + b_{i+1}|\phi_{i+1}\rangle, \quad 1 \leq i \leq M. \quad (45)$$

By stopping the iteration at  $i = M$  and putting the last coefficient  $b_{M+1} = 0$ , the Hamiltonian can be represented in the basis of orthogonal Lanczos functions  $|\phi_i\rangle$  as the tridiagonal matrix  $H_M$  with diagonal elements  $a_i$  with  $i = 0 \dots M$ , and offdiagonal ones  $b_i$  with  $i = 1 \dots M$ . Such a matrix is easily diagonalized using standard numerical routines to obtain approximate eigenvalues  $\epsilon_j$  and the corresponding orthonormal eigenvectors  $|\psi_j\rangle$ ,

$$|\psi_j\rangle = \sum_{i=0}^M v_{ji}|\phi_i\rangle, \quad j = 0 \dots M. \quad (46)$$

It is important to realize that  $|\psi_j\rangle$  are (in general) not exact eigenfunctions of  $H$ , but show a remainder

$$H|\psi_j\rangle - \epsilon_j|\psi_j\rangle = b_{M+1}v_{jM}|\phi_{M+1}\rangle. \quad (47)$$

On the other hand it is evident from the diagonalization of  $H_M$  that matrix elements

$$\langle\psi_i|H|\psi_j\rangle = \epsilon_j\delta_{ij}, \quad i, j = 0 \dots M \quad (48)$$

are exact, without restriction to the subspace  $L_M$ .

The identity (48) already shows the usefulness of the Lanczos method for the calculation of particular matrix elements. As an aid in a further discussion of the Lanczos method we consider the calculation of a matrix element

$$W_{kl} = \langle n|H^k B H^l A|n\rangle, \quad (49)$$



where  $|n\rangle$  is an arbitrary normalized vector, and  $A, B$  are general operators. One can calculate this expression exactly by performing two Lanczos procedures with  $M = \max(k, l)$  steps. The first one, starting with the vector  $|\phi_0\rangle = |n\rangle$ , produces the subspace  $L_M = \{|\phi_j\rangle, j = 0 \dots M\}$  along with approximate eigenvectors  $|\psi_j\rangle$  and eigenvalues  $\varepsilon_j$ . The second Lanczos procedure is started with the normalized vector

$$|\tilde{\phi}_0\rangle = A|\phi_0\rangle / \sqrt{\langle\phi_0|A^\dagger A|\phi_0\rangle}, \quad (50)$$

and results in the subspace  $\tilde{L}_M = \{|\tilde{\phi}_j\rangle, j = 0 \dots M\}$  with approximate  $|\tilde{\psi}_j\rangle$  and  $\tilde{\varepsilon}_j$ . We can now define projectors

$$P_m = \sum_{i=0}^m |\phi_i\rangle\langle\phi_i|, \quad \tilde{P}_m = \sum_{i=0}^m |\tilde{\phi}_i\rangle\langle\tilde{\phi}_i|, \quad (51)$$

which for  $m = M$  can also be expressed as

$$P_M = \sum_{i=0}^M |\psi_i\rangle\langle\psi_i|, \quad \tilde{P}_M = \sum_{i=0}^M |\tilde{\psi}_i\rangle\langle\tilde{\psi}_i|. \quad (52)$$

By taking into account definitions (51), (52) we show that

$$HP_m = P_{m+1}HP_m = P_MHP_m, \quad m < M. \quad (53)$$

Since in addition  $|n\rangle = |\phi_0\rangle = P_0|\phi_0\rangle$  and  $A|n\rangle \propto |\tilde{\phi}_0\rangle = P_0|\tilde{\phi}_0\rangle$ , by successive use of the first equality in (53) we arrive at

$$W_{kl} = \langle\phi_0|P_MHP_MH \dots HP_MB\tilde{P}_MH \dots \tilde{P}_MH\tilde{P}_MA|\phi_0\rangle. \quad (54)$$

We note that the necessary condition for the equation (54) is  $M \geq k, l$ . We finally expand the projectors according to expressions (52) and take into account the orthonormality relation (48) for matrix elements, and get

$$\begin{aligned} W_{kl} &= \sum_{i_0=0}^M \dots \sum_{i_k=0}^M \sum_{j_0=0}^M \dots \sum_{j_l=0}^M \langle\phi_0|\psi_{i_0}\rangle\langle\psi_{i_0}|H|\psi_{i_1}\rangle \dots \langle\psi_{i_{k-1}}|H|\psi_{i_k}\rangle \\ &\quad \times \langle\psi_{i_k}|B|\tilde{\psi}_{j_l}\rangle\langle\tilde{\psi}_{j_l}|H|\tilde{\psi}_{j_{l-1}}\rangle \dots \langle\tilde{\psi}_{j_1}|H|\tilde{\psi}_{j_0}\rangle\langle\tilde{\psi}_{j_0}|A|\phi_0\rangle = \\ &= \sum_{i=0}^M \sum_{j=0}^M \langle\phi_0|\psi_i\rangle\langle\psi_i|B|\tilde{\psi}_j\rangle\langle\tilde{\psi}_j|A|\phi_0\rangle(\varepsilon_i)^k(\tilde{\varepsilon}_j)^l. \end{aligned} \quad (55)$$

We have thus expressed the desired quantity in terms of the Lanczos (approximate) eigenvectors and eigenvalues alone.

Within the Lanczos algorithm the extreme (smallest and largest) eigenvalues  $\varepsilon_i$ , along with their corresponding  $|\psi_i\rangle$ , are rapidly converging to exact eigenvalues  $E_i$  and eigenvectors  $|\Psi_i\rangle$ . It is quite characteristic that usually (for nondegenerate states)  $M = 30 - 60 \ll N_{st}$  is sufficient to achieve the convergence to the machine precision of

the ground state energy  $E_0$  and the wavefunction  $|\Psi_0\rangle$ , from which various static and dynamical correlation functions at  $T = 0$  can be evaluated.

After  $|\Psi_0\rangle$  is obtained, the g.s. dynamic correlation functions can be calculated within the same framework [15]. Let us consider the autocorrelation function

$$C(t) = -i\langle\Psi_0|A^\dagger(t)A|\Psi_0\rangle = -i\langle\Psi_0|A^\dagger e^{i(E_0-H)t}A|\Psi_0\rangle \quad (56)$$

with the transform,

$$\tilde{C}(\omega) = \int_0^\infty dt e^{i\omega^+ t} C(t) = \langle\Psi_0|A^\dagger \frac{1}{\omega^+ + E_0 - H} A|\Psi_0\rangle. \quad (57)$$

To calculate  $\tilde{C}(\omega)$ , one has to run the second Lanczos procedure starting with the normalized function  $|\tilde{\phi}_0\rangle$ , equation (50). The matrix for  $H$  in the new basis  $\tilde{L}_M$ , with elements  $\langle\tilde{\phi}_i|H|\tilde{\phi}_j\rangle = [\tilde{H}_M]_{ij}$ , is again a tridiagonal one with  $\tilde{a}_i$  and  $\tilde{b}_i$  elements, respectively. Terminating the Lanczos procedure at given  $M$ , one can evaluate the  $\tilde{C}(\omega)$  as a resolvent of the  $\tilde{H}_M$  matrix which can be expressed in the continued-fraction form [15],

$$\tilde{C}(\omega) = \frac{\langle\Psi_0|A^\dagger A|\Psi_0\rangle}{\omega^+ + E_0 - \tilde{a}_0 - \frac{\tilde{b}_1^2}{\omega^+ + E_0 - \tilde{a}_1 - \frac{\tilde{b}_2^2}{\omega^+ + E_0 - \tilde{a}_2 - \dots}}}, \quad (58)$$

terminating with  $\tilde{b}_{M+1} = 0$ , although other termination functions have also been employed.

The spectral function  $C(\omega) = -(1/\pi)\text{Im}\tilde{C}(\omega)$  is characterized by frequency moments,

$$\mu_l = \int_{-\infty}^\infty \omega^l C(\omega) d\omega = \langle\Psi_0|A^\dagger (H - E_0)^l A|\Psi_0\rangle, \quad (59)$$

which are particular cases of the expression (49) for  $B = A^\dagger$ ,  $k = 0$ , and  $|n\rangle = |\Psi_0\rangle$ . Using the equation (55) we can express  $\mu_l$  for  $l \leq M$  in terms of Lanczos quantities alone

$$\mu_l = \sum_{j=0}^M \langle\Psi_0|A^\dagger|\tilde{\psi}_j\rangle \langle\tilde{\psi}_j|A|\Psi_0\rangle (\tilde{\epsilon}_j - E_0)^l. \quad (60)$$

Hence moments  $\mu_{l < M}$  are exact for given  $|\Psi_0\rangle$ .

## Finite temperature Lanczos method

The novel method for  $T > 0$  [16, 17] is based on the application of the Lanczos iteration, reproducing correctly high- $T$  and large- $\omega$  series. The method is then combined with the reduction of the full thermodynamic trace to the random sampling.

We first consider the expectation value of the operator  $A$  in the canonical ensemble

$$\langle A \rangle = \sum_{n=1}^{N_{st}} \langle n | e^{-\beta H} A | n \rangle \bigg/ \sum_{n=1}^{N_{st}} \langle n | e^{-\beta H} | n \rangle. \quad (61)$$

A straightforward calculation of  $\langle A \rangle$  requires the knowledge of all eigenstates  $|\Psi_n\rangle$  and corresponding energies  $E_n$ , obtained by the full diagonalization of  $H$ , computationally accessible only for  $N_{st} < 3000$ . Instead let us perform the high-temperature expansion of the exponential  $\exp(-\beta H)$ ,

$$\begin{aligned}\langle A \rangle &= Z^{-1} \sum_{n=1}^{N_{st}} \sum_{k=0}^{\infty} \frac{(-\beta)^k}{k!} \langle n | H^k A | n \rangle, \\ Z &= \sum_{n=1}^{N_{st}} \sum_{k=0}^{\infty} \frac{(-\beta)^k}{k!} \langle n | H^k | n \rangle.\end{aligned}\quad (62)$$

Terms in the expansion  $\langle n | H^k A | n \rangle$  can be calculated exactly using the Lanczos procedure with  $M \geq k$  steps and with  $|\phi_0^n\rangle = |n\rangle$  as a starting function, since this is a special case of the expression (49). Using the relation (55) with  $l = 0$  and  $B = 1$ , we get

$$\langle n | H^k A | n \rangle = \sum_{i=0}^M \langle n | \psi_i^n \rangle \langle \psi_i^n | A | n \rangle (\epsilon_i^n)^k. \quad (63)$$

Working in a restricted basis  $k \leq M$ , we can insert the expression (63) into sums (62), extending them to  $k > M$ . The final result can be expressed as

$$\begin{aligned}\langle A \rangle &\approx Z^{-1} \sum_{n=1}^{N_{st}} \sum_{i=0}^M e^{-\beta \epsilon_i^n} \langle n | \psi_i^n \rangle \langle \psi_i^n | A | n \rangle, \\ Z &\approx \sum_{n=1}^{N_{st}} \sum_{i=0}^M e^{-\beta \epsilon_i^n} \langle n | \psi_i^n \rangle \langle \psi_i^n | n \rangle,\end{aligned}\quad (64)$$

and the error of the approximation is of the order of  $\beta^{M+1}$ .

Evidently, within a finite system the expression (64), expanded as a series in  $\beta$ , reproduces exactly the high- $T$  expansion series to the order  $M$ . In addition, in contrast to the usual series expansion, it becomes (remains) exact also for  $T \rightarrow 0$ . Let us assume for simplicity that the ground state  $|\Psi_0\rangle$  is nondegenerate. For initial states  $|n\rangle$  not orthogonal to  $|\Psi_0\rangle$ , already at modest  $M < 60$  the lowest function  $|\psi_0^n\rangle$  converges to  $|\Psi_0\rangle$ . Eq.(64) for  $\beta \rightarrow \infty$  then gives,

$$\begin{aligned}\langle A \rangle &= \sum_{n=1}^{N_{st}} \langle n | \Psi_0 \rangle \langle \Psi_0 | A | n \rangle / \sum_{n=1}^{N_{st}} \langle n | \Psi_0 \rangle \langle \Psi_0 | n \rangle = \\ &= \langle \Psi_0 | A | \Psi_0 \rangle / \langle \Psi_0 | \Psi_0 \rangle,\end{aligned}\quad (65)$$

where we have taken into account the completeness of the set  $|n\rangle$ . Obtained result is just the usual ground state expectation value of an operator.

In order to calculate dynamical quantities, the high- $T$  expansion must be supplemented by the high-frequency (short-time) expansion. The goal is to calculate the dynamical correlation function at  $T > 0$ ,

$$\langle B(t)A \rangle = \text{Tr} \left[ e^{-\beta H} e^{iHt} B e^{-iHt} A \right] / \text{Tr} e^{-\beta H}. \quad (66)$$

Expressing the trace explicitly and expanding the exponentials, we get

$$\langle B(t)A \rangle = Z^{-1} \sum_{n=1}^{N_{st}} \sum_{k=0}^{\infty} \sum_{l=0}^{\infty} \frac{(-\beta + it)^k}{k!} \frac{(-it)^l}{l!} \langle n | H^k B H^l A | n \rangle. \quad (67)$$

Expansion coefficients in equation (67) can be again obtained via the Lanczos method. Performing two Lanczos iterations with  $M$  steps, started with normalized  $|\phi_0^n\rangle = |n\rangle$  and  $|\tilde{\phi}_0^n\rangle \propto A|n\rangle$ , respectively, we calculate coefficients  $W_{kl}$  following the equation (55), while  $Z$  is approximated by the static expression (64). Extending and resumming series in  $k$  and  $l$  into exponentials, we get

$$\langle B(t)A \rangle \approx Z^{-1} \sum_{n=1}^{N_{st}} \sum_{i=0}^M \sum_{j=0}^M e^{-\beta \epsilon_i^n} e^{it(\epsilon_i^n - \tilde{\epsilon}_j^n)} \langle n | \Psi_i^n \rangle \langle \Psi_i^n | B | \tilde{\Psi}_j^n \rangle \langle \tilde{\Psi}_j^n | A | n \rangle. \quad (68)$$

The computation of static quantities (64) and dynamical ones (68) still involves the summation over the complete set of  $N_{st}$  states  $|n\rangle$ , which is not feasible in practice. To obtain a useful method, one further approximation must be made which replaces the full summation by a partial one over a much smaller set of random states. Such an approximation, analogous to Monte Carlo methods, is of course hard to justify rigorously, nevertheless we can estimate the errors involved.

We consider the expectation value  $\langle A \rangle$  at  $T > 0$ , as defined by the expression (61). Instead of the whole sum in equation (61) we first evaluate only one element with respect to a random state  $|r\rangle$ , which is a linear combination of basis states

$$|r\rangle = \sum_{n=1}^{N_{st}} \beta_{rn} |n\rangle, \quad (69)$$

i.e.  $\beta_{rn}$  are assumed to be distributed randomly. Let us discuss then the random quantity

$$\tilde{A}_r = \langle r | e^{-\beta H} A | r \rangle / \langle r | e^{-\beta H} | r \rangle \quad (70)$$

We express  $|\beta_{rn}|^2 = 1/N_{st} + \delta_{rn}$  and assume that random deviations  $\delta_{rn}$  are not correlated with matrix elements  $\langle n | e^{-\beta H} | n \rangle = Z_n$  and  $\langle n | e^{-\beta H} A | n \rangle = Z_n A_n$ . Then it is easy to show that  $\tilde{A}_r$  is close to  $\langle A \rangle$ , and the statistical deviation is related to the effective number of terms  $\bar{Z}$  in the thermodynamic sum, i.e.

$$\tilde{A}_r = \langle A \rangle + o(1/\sqrt{\bar{Z}}), \quad \bar{Z} = e^{\beta E_0} \sum_n Z_n \sim \text{Tre}^{-\beta(H-E_0)}. \quad (71)$$

Note that for  $T \rightarrow \infty$  we have  $\bar{Z} \rightarrow N_{st}$  and therefore at large  $N_{st}$  a close estimate of the average (71) can be obtained from a single random state. On the other hand, at finite  $T < \infty$  the statistical error of  $\tilde{A}_r$  increases with decreasing  $\bar{Z}$ . In the FTLM we replace the full summation in the expression (61) with a restricted one over several random vectors  $|r\rangle$ ,  $r = 1, R$  and the statistical error is even reduced,

$$\tilde{A} = \langle A \rangle + o(1/\sqrt{R\bar{Z}}). \quad (72)$$

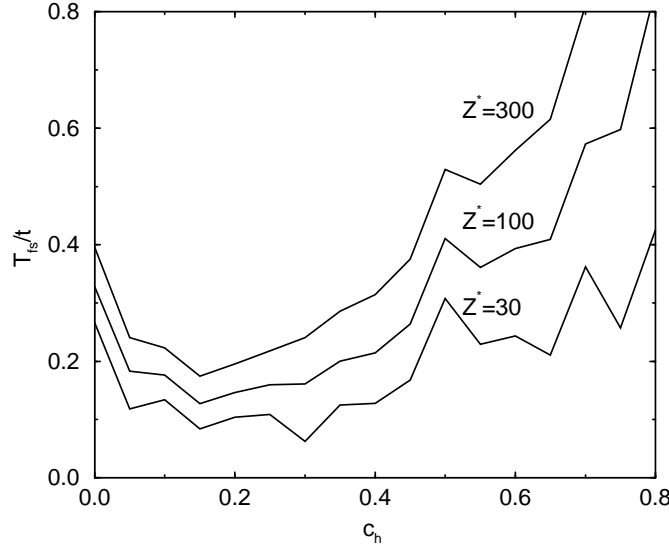


**FIGURE 5.** The variation of  $T_{fs}$  with doping  $c_h$  in the  $t$ - $J$  on  $N = 18$  sites with  $J/t = 0.3$ . Curves correspond to different choices of  $Z^* = \bar{Z}(T_{fs})$ .

We introduce and justify the finite-temperature Lanczos method as a method to calculate  $T > 0$  properties on small systems, but as well as a controlled approach to results at  $T \rightarrow 0$  in the thermodynamic limit. We also argue that choosing appropriate  $M$ , and the sampling  $R$  one can reproduce exact results to prescribed precision on a given system. The well known deficiency of the exact diagonalization methods is however the smallness of available lattices, hence it is important to understand the finite size effects and their role at  $T > 0$ . We claim that generally  $T > 0$  reduces finite size effects. This is related to the fact that at  $T = 0$  both static and dynamical quantities are calculated only from one wavefunction  $|\Psi_0\rangle$ , which can be quite dependent on the size and on the shape of the system.  $T > 0$  introduces the thermodynamic averaging over a larger number of eigenstates. This reduces directly finite-size effects for static quantities, whereas for dynamical quantities spectra become denser.

The effect of  $T > 0$  can be expressed also in another way. There are several characteristic length scales in the system of correlated electrons, e.g. the antiferromagnetic correlation length  $\xi$ , the transport mean free path  $l_s$ , etc. These lengths decrease with increasing  $T$  and results for related quantities have a macroscopic relevance provided that the lengths become shorter than the system size, e.g.  $l_s < L$  where  $L$  is the linear size of the system. This happens for particular  $T > T_s$ , where clearly  $T_s$  depends also on the quantity considered.

As a criterion for finite size effects we use the characteristic finite-size temperature  $T_{fs}$ . It is chosen so that in a given system the thermodynamic sum in Eq.(71) is appreciable, i.e.  $\bar{Z}(T_{fs}) = Z^* \gg 1$ . The finite-temperature Lanczos method is thus best suited just for quantum many-body systems with a large degeneracy of states, i.e. large  $\bar{Z}$  at low  $T$ . This is the case with doped antiferromagnet and the  $t$ - $J$  model in the strong correlation

regime  $J < t$ . To be concrete we present in Fig. 5 the variation of  $T_{fs}$  with the doping  $c_h = N_h/N$ , as calculated from the system of  $N = 18$  sites and  $J/t = 0.3$ . It is indicative that  $T_{fs}$  reaches the minimum for intermediate (optimum) doping  $c_h = c_h^* \sim 0.15$ . Away from such optimum case  $T_{fs}$  is larger. We claim that small  $T_{fs}$  and related large degeneracy of low-lying states are the essential features of strongly correlated system in their most challenging regime (so called underdoped and optimally doped regime of cuprates), being a sign of a novel quantum frustration. This is consistent with the experimental results on cuprates, where the optimal doping with respect to  $T_c$  coincides with largest degeneracy, i.e. electronic entropy density  $s$ .

## **$T$ - $J$ MODEL VS. CUPRATES**

The main motivation to understand transport in strongly correlated systems comes from the well established anomalous properties of high- $T_c$  cuprates, whereby in our context we consider only the "normal" metallic state. The prominent example is nearly linear in-plane resistivity  $\rho \propto T$  in the normal state [4]. It is however an experimental fact that such a behaviour is restricted to the optimum doping regime, while deviations from linearity appear both in the underdoped and overdoped regimes, being still universal for a number of materials with a similar doping. The d.c. resistivity  $\rho$  is intimately related to the optical conductivity  $\sigma(\omega)$ , which has been also extensively studied and shows in the normal state the unusual non-Drude behaviour fitted with the marginal Fermi-liquid [18] behaviour  $\tau \sim 2\pi\lambda(\omega + \xi T)$ .

There is a lot of evidence that the anomalous electrical transport in cuprates is mainly due to strong correlations. Moreover, it seems that at least within the normal metallic state the physics of cuprates can be well captured within the single-band  $t$ - $J$  model, the simplest model which contains the interplay of the charge propagation and spin (antiferromagnetic) exchange,

$$H = -t \sum_{\langle ij \rangle s} (\tilde{c}_{js}^\dagger \tilde{c}_{is} + \text{H.c.}) + J \sum_{\langle ij \rangle} (\mathbf{S}_i \cdot \mathbf{S}_j - \frac{1}{4} n_i n_j). \quad (73)$$

Here  $\mathbf{S}_i$  are the local spin operators interacting with the exchange parameter  $J$ . Due to the strong on-site repulsion the double occupation of sites is explicitly forbidden and we are dealing with projected fermion operators  $\tilde{c}_{is} = c_{is}(1 - n_{i,-s})$ .

Due to small number of local degrees of freedom ( $N_i = 3$ ) the  $t$ - $J$  model is particularly convenient for studies with the exact diagonalization method. Ground state properties of the planar model on a square lattice have been intensively investigated [6], more recently also the  $T > 0$  properties using the finite-temperature Lanczos method [17].

Let us go straight to results at the intermediate (optimum) doping, where we can reach lowest  $T_{fs}$ . Instead of  $\sigma(\omega)$  directly it is more instructive to present the current correlation function  $C(\omega)$ , equation (12). To avoid the ambiguities with an additional smoothing, we plot the corresponding integrated spectra

$$I_C(\omega) = \int_0^\omega C(\omega') d\omega'. \quad (74)$$

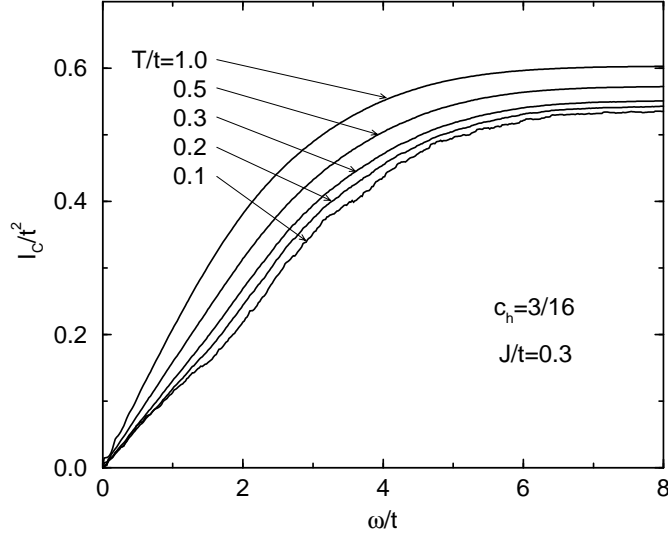


**FIGURE 6.** Integrated current correlation spectra  $I_C(\omega)$  at  $c_h = 3/16$  for different  $T \leq t$ .

In Fig. 6 we present  $I_C(\omega)$  for the intermediate (optimal) doping  $c_h = 3/16$ , for various  $T \leq t$ . Spectra reveal several remarkable features [17]:

a) For  $T \leq J$  spectra  $I_C(\omega)$  are essentially independent of  $T$ , at least for available  $T > T_{fs}$ .

b) Simultaneously the slope of  $I_C(\omega < 2t)$  is nearly constant, i.e. we find  $C(\omega) \sim C_0$  in a wide range  $\omega < 2t$ . At the same time  $C_0$  is only weakly dependent on  $J$  as tested for  $J/t = 0.2 - 0.6$ .

c) Even for higher  $T > J$  the differences in the slope  $C_0$ , as also in  $I_C(\infty)$ , appear as less essential.

We conclude that  $C(\omega < 2t) \sim C_0$  implies a simple universal form,

$$\sigma(\omega) = C_0 e_0^2 \frac{1 - e^{-\beta\omega}}{\omega}. \quad (75)$$

Such a  $\sigma(\omega)$  shows a nonanalytic behaviour at  $\omega \rightarrow 0$ , starting with a finite slope. This is already an indication that  $\sigma(\omega)$  is not consistent with the usual Drude form, but rather with a marginal concept [18] where the only  $\omega$  scale is given by  $T$ . It is also remarkable that the form (75) trivially reproduces the linear law  $\rho \propto T$  as well as the non-Drude fall-off at  $\omega > T$ . It is evident that the expression (75) is universal containing the only parameter  $C_0$  as a prefactor.

Experimental results and theoretical considerations are often discussed in terms of the  $\omega$ -dependent relaxation time  $\tau$  and the effective mass  $m^*$ . These can be uniquely introduced via the complex  $\tilde{\sigma}(\omega)$  and the corresponding memory function  $M(\omega)$ ,

$$\tilde{\sigma}(\omega) = \frac{ie_0^2 S}{\omega + M(\omega)}, \quad S = -\langle H_{kin} \rangle / 2N, \quad (76)$$

and

$$\begin{aligned}\frac{1}{\tau(\omega)} &= \frac{M''(\omega)}{1 + M'(\omega)/\omega}, \\ \frac{m^*(\omega)}{m_t} &= \frac{2c_h t}{s} \left( 1 + \frac{M'(\omega)}{\omega} \right),\end{aligned}\quad (77)$$

where  $m_t = 1/2ta_0^2$  is the bare band mass. Using relations (76),(77) one can formally rewrite  $\tilde{\sigma}(\omega)$  in the familiar Drude form

$$\tilde{\sigma}(\omega) = \frac{ic_h e_0^2}{m^*(\omega)[\omega + i/\tau(\omega)]}. \quad (78)$$

Employing the equation (78) we evaluate both  $\tau(\omega)$  and  $m^*(\omega)$  from known  $\tilde{\sigma}(\omega)$ . It follow directly from the form (75), that in the regime  $T < J$  and  $\omega < t$  we can describe the behaviour of  $1/\tau$  with a linear law

$$\tau^{-1} = 2\pi\lambda(\omega + \xi T), \quad \lambda \sim 0.09, \quad \xi \sim 2.7. \quad (79)$$

This dependence falls within the general framework of the marginal Fermi liquid scenario [18]. It should be however stressed that the asymptotic form (79) does not allow for any free parameter, i.e. constants  $\lambda$  and  $\xi$  are universal and independent of any model parameters, whereas within the original marginal Fermi-liquid proposal  $\lambda$  is an adjustable parameter while  $\xi = \pi$ .

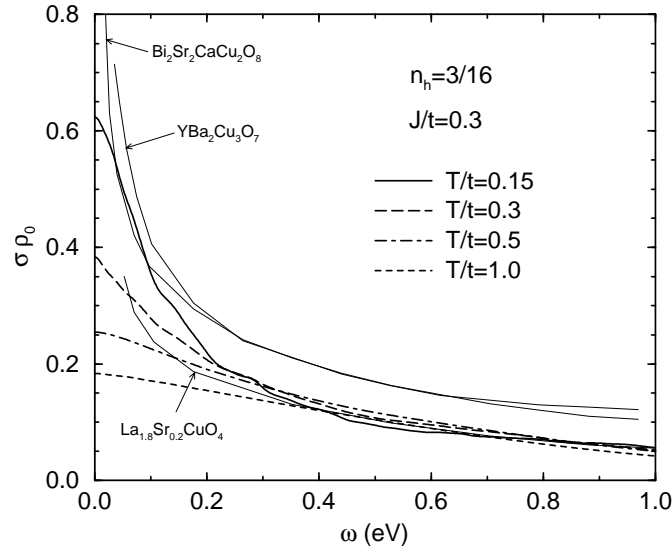


**FIGURE 7.** Sheet conductivities  $\sigma(\omega)$  for various  $T/t$ , in comparison with measurements in different cuprates. Experimental results refer to  $T < 200$  K.

Let us relate obtained model results to experimets in cuprates. Since parameters of the model, corresponding to cuprates, are to large extent known, i.e.  $J/t \sim 0.3$



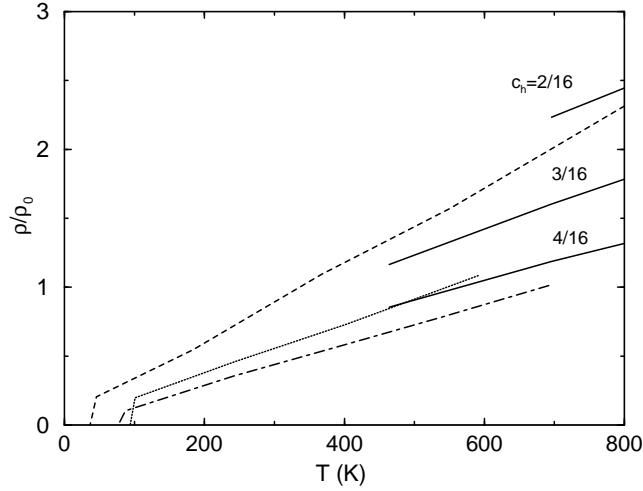


**FIGURE 8.** Sheet resistivities  $\rho(T)$  for various dopings (full lines) in comparison with measurements in LSCO with  $x = 0.15$  (dotted), BSCCO (dashed), and YBCO (dash-dotted).

and  $t \sim 0.4\text{eV}$ , the direct comparison of  $\sigma(\omega)$  and  $\rho(T)$  can be performed without any additional assumptions. In 2D  $\sigma$  is naturally expressed in terms of the universal constant  $\rho_0 = \hbar/e_0^2$ . The corresponding 3D conductivity of a stack of 2D conducting sheets with an average distance  $\bar{c}$  is given instead by  $\sigma_{3D} = \sigma/\bar{c}$ . For comparison with experiments we reduce the 3D measured values to the 2D conductivities for three different cuprates at intermediate doping, i.e.  $\text{La}_{2-x}\text{Sr}_x\text{CuO}_4$  (LSCO) with  $x = 0.2$ ,  $\text{Bi}_2\text{Sr}_2\text{CaCu}_2\text{O}_{8+\delta}$  (BSCCO) and  $\text{YBa}_2\text{Cu}_3\text{O}_7$  (YBCO). Taking into account the uncertainty in effective hole doping within these materials calculated spectra  $\sigma(\omega)$  for  $c_h = 3/16$  are in a quantitative agreement with measurements, as seen in Fig. 7. It should be noted that also calculated  $\tau^{-1}(\omega)$  and corresponding parameters  $\lambda$  and  $\xi$ , as defined by the equation (79) are close to the experimental ones.

In Fig. 8 we compare calculated  $\rho(T)$  to the measured ones. It should be pointed out that there is a restricted  $T$  window where a comparison could be made since  $T_{fs} \sim 450\text{K}$ , whereby at  $T \sim T_{fs}$  also finite-size effects start to influence our analysis. Nevertheless, for the intermediate doping  $c_h \sim 0.2$  our  $\rho(T)$  results match quantitatively well experimental ones for cuprates with comparable hole concentrations, i.e. for BSCCO, YBCO and LSCO with  $x = 0.15$ .

## Origin of anomalous conductivity

There is so far no accepted explanation for the origin of the anomalous marginal-type charge dynamics in cuprates. From our analysis of the  $t$ - $J$  model at the intermediate doping it seems to be quite generic feature of frustrated regime of correlated electrons. In the following we try to argue that there is in general a relation between the marginal-type  $\sigma(\omega)$  and the overdamped character of quasiparticle excitations, also observed

experimentally in cuprates via the angle-resolved photoemission spectroscopy (ARPES) as well in model studies.

Let us perform for  $C(\omega)$  the decoupling in terms of single-particle (electron) spectral functions  $A(\mathbf{k}, \omega)$  neglecting possible vertex corrections, i.e.

$$C(\omega) = \frac{2\pi e_0^2}{N} \sum_{\mathbf{k}} (v_{\mathbf{k}}^\alpha)^2 \int d\omega' f(-\omega') f(\omega' - \omega) A(\mathbf{k}, \omega') A(\mathbf{k}, \omega' - \omega), \quad (80)$$

where  $f(\omega)$  are Fermi functions and  $v_{\mathbf{k}}^\alpha$  are (unrenormalized) band-velocity components. While such an approach is usual in weak scattering problems, qualitative features could be reasonable also for strongly correlated electrons. We assume also that  $A(\mathbf{k}, \omega)$  for quasiparticles close to the Fermi energy ( $\omega = 0$ ) can be generally presented as

$$A(\mathbf{k}, \omega) = \frac{1}{\pi} \frac{Z_{\mathbf{k}} \Gamma_{\mathbf{k}}}{(\omega - \epsilon_{\mathbf{k}})^2 + \Gamma_{\mathbf{k}}^2}, \quad (81)$$

where quasiparticle parameters  $Z_{\mathbf{k}}, \Gamma_{\mathbf{k}}, \epsilon_{\mathbf{k}}$  can still be dependent on  $\omega$  and  $T$ . In order to reproduce the marginal Fermi liquid form, Eqs.(78),(79), of  $\sigma(\omega)$  we have to postulate an analogous form also for the quasiparticle damping, i.e.  $\Gamma = \gamma(|\omega| + \xi T)$  (consistent with recent ARPES experiments in BSCCO), but we neglect the  $\mathbf{k}$  dependence of  $\Gamma$  and  $Z$ .

For  $\omega < \omega^*$ , whereby the cutoff  $\omega^*$  appears due to the effective bandwidth or some other characteristic quasiparticle scale, only the behavior near the Fermi surface should be important. Replacing in Eq.(80) the  $\mathbf{k}$  summation with an integral over  $\epsilon$  with a slowly varying density of states  $\mathcal{N}(\epsilon)$  one can derive

$$\int d\epsilon A(\epsilon, \omega') A(\epsilon, \omega' - \omega) = \frac{Z^2}{\pi} \frac{\bar{\Gamma}(\omega, \omega')}{\omega^2 + \bar{\Gamma}(\omega, \omega')^2}, \quad (82)$$

where  $\bar{\Gamma}(\omega, \omega') = \Gamma(\omega') + \Gamma(\omega' - \omega)$ . We are thus dealing with a function  $C(\omega)$ ,

$$C(\omega) = \bar{C} \int d\omega' f(-\omega') f(\omega' - \omega) \frac{\bar{\Gamma}(\omega, \omega')}{\omega^2 + \bar{\Gamma}(\omega, \omega')^2}, \quad (83)$$

depending only on the ratio  $\omega/T$ , and on the parameters  $\gamma, \xi$ . In the theory of Fermi liquids  $\omega$  and  $T$  variation are tightly bound so  $\xi$  should also be quite universal or at least quite restricted in range, whereby  $\xi \sim \pi$  is usually used [18].

It is evident from Eq.(83) that for  $\gamma \ll 1$  we recover  $C(\omega)$  strongly peaked at  $\omega = 0$  and consequently  $\sigma(\omega) \propto \bar{\Gamma}/(\omega^2 + \bar{\Gamma}^2)$  with  $\bar{\Gamma} = 2\Gamma(\omega/2, T)$ . This is just a generalized Drude form with  $1/\tau(\omega) = 2\Gamma(\omega/2)$ .  $\sigma(\omega)$  is in this case directly determined by the single-particle relaxation  $\Gamma$ .

This relation is however not valid when one approaches the regime of overdamped QP excitations  $\gamma \sim 1$  or more appropriate  $\gamma\xi \sim 1$ . We present in Fig. 9 results for  $C(\omega)$  for several  $\gamma$  fixing  $\xi = \pi$ . While for  $\gamma < 0.2$  still a pronounced peak shows up at  $\omega \sim 0$ ,  $C(\omega)$  becomes for  $\gamma > 0.3$  nearly constant or very slowly varying in a wide range of  $\omega/T$ . For large  $\gamma$  we find even  $C(0) < C(\omega \rightarrow \infty)$ , approaching for  $\gamma \gg 1$  the ratio  $C(0)/C(\infty) = 1/\xi$ .

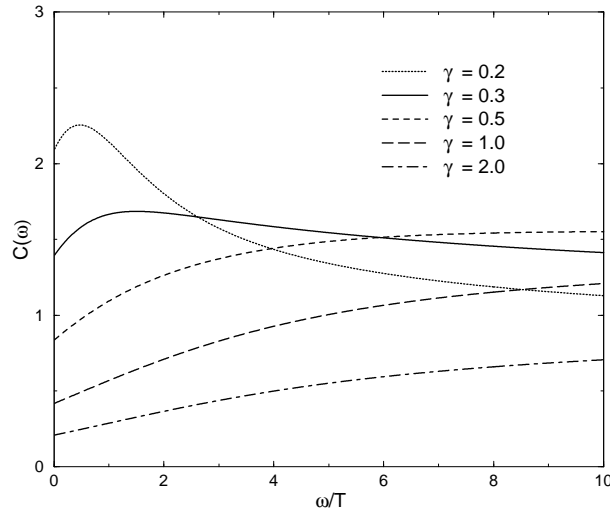


**FIGURE 9.** Current-current correlation spectra  $C(\omega)$  vs.  $\omega/T$  for various  $\gamma$  at fixed  $\xi = \pi$ .

The main message of the above simple analysis is that for systems with overdamped quasiparticle excitations of the marginal Fermi-liquid form the expression Eq.(75) describes quite well  $\sigma(\omega)$  for a wide range of parameters. It should be stressed that nearly constant  $C(\omega < \omega^*)$  also means that the current relaxation rate  $1/\tau^*$  is very fast,  $1/\tau^* \sim \omega^* \gg 1/\tau$ , i.e. much faster than the conductivity relaxation scale apparent from Eq.(79) where  $1/\tau \propto T$  is determined solely by thermodynamics.

## CONCLUSIONS

The theory of electron transport in models and materials dominated by strong electron-electron repulsion is still in its infancy. Present lectures try to describe some of novel phenomena in transport, which seem to be particular to correlated systems. At the same time it is evident that there are even more open problems which wait for proper theoretical understanding and feasible methods for systematic study:

a) The singular transport in nontrivial integrable models of interacting fermions reveal an evident question which are relevant scattering processes which determine transport quantities. Coulomb repulsion and Umklapp processes are in general clearly not enough to lead to current relaxation and dissipation. As shown in integrable systems transport quantities remain singular. It is expected that in general any deviation from integrability will lead to a normal resistance, however there exists no reliable approach to transport in the vicinity of integrable points.

b) Even in integrable 1D systems there are several open questions. Although the relation to conserved quantities is very appealing and more operational it is questionable whether it can explain generally the existence of ideal conductors, e.g. the ideal conductor in the simplest cases as the  $t$ - $V$  model at half filling, the particle in the fermionic bath etc.

c) The existence of very unusual ideal insulator has not been proven nor disproven yet.

d) For higher dimensional systems there is definite need for analytical methods which would allow the evaluation of (at least qualitatively correct) transport quantities. Recently developed numerical methods for finite correlated systems, in particular the finite-temperature Lanczos method, have proven to be very useful. Their weakness is clearly in the smallness of reachable systems. Fortunately, the physics in several relevant models appears to be quite local in character so that e.g. mean free path is very short even at moderately low temperatures.

e) The main motivation to study correlated systems comes from the observation of anomalous conductivity  $\sigma(\omega)$  in high- $T_c$  cuprates as prominent example of materials with strongly correlated electrons. Numerical studies as well as analytical relation with spectral functions with overdamped quasiparticles confirm the observed behavior described within the marginal Fermi liquid scenario. These materials seem to follow a novel quantum diffusion law where relaxation is dominated by thermodynamics only. However its origin is not well understood. Also it is not clear how general such scenario might be and whether (why) it breaks down at low enough temperatures.

## REFERENCES

1. G.D. Mahan, *Many-Particle Physics* (Plenum, New York) (1990).
2. W. Kohn, Phys. Rev. **133**, A171 (1964).
3. P.F. Maldague, Phys. Rev. B **16**, 2437 (1977).
4. for a review see, e.g., M. Imada, A. Fujimori, and Y. Tokura, Rev. Mod. Phys. **70**, 1039 (1998).
5. A. Georges, G. Kotliar, W. Krauth, and M.J. Rozenberg, Rev. Mod. Phys. **68**, 13 (1996).
6. E. Dagotto, Rev. Mod. Phys. **66**, 763 (1994).
7. X. Zotos and P. Prelovšek, Phys. Rev. B **53**, 983 (1996).
8. H. Castella and X. Zotos, P. Prelovšek, Phys. Rev. Lett. **74**, 972 (1995).
9. D. Poilblanc, T. Ziman, J. Bellisard, F. Mila, and G. Montambaux, Europhys. Lett. **22**, 537 (1993).
10. M. Wilkinson, J. Phys. A : Math. Gen. **21**, 4021 (1988); Phys. Rev. A **41**, 4645 (1990).
11. H. Castella, X. Zotos, Phys. Rev. B **47**, 16186 (1993).
12. P. Mazur, Physica **43**, 533 (1969).
13. M. Suzuki, Physica **51**, 277 (1971).
14. B.N. Partlett, *The Symmetric Eigenvalue Problem* (Prentice Hall, Englewood Cliffs) (1980).
15. R. Haydock, V. Heine, and M.J. Kelly, J. Phys. C **5**, 1845 (1972).
16. J. Jaklič and P. Prelovšek, Phys. Rev. B **49**, 5065 (1994).
17. for a review see J. Jaklič and P. Prelovšek, Adv. Phys. **49**, 1 (2000).
18. C.M. Varma *et al.*, Phys. Rev. Lett. **63**, 1996 (1989).